PHILOSOPHICAL TRANSACTIONS OF THE ROYAL SOCIETY B BIOLOGICAL SCIENCES

Flight Performance and Visual Control of Flight of the Free-Flying Housefly (Musca Domestica L.) I. Organization of the Flight Motor

H. Wagner

Phil. Trans. R. Soc. Lond. B 1986 **312**, 527-551
doi: 10.1098/rstb.1986.0017

Phil. Trans. R. Soc. Lond. B **312**, 527–551 (1986) [527]
Printed in Great Britain

FLIGHT PERFORMANCE AND VISUAL CONTROL OF FLIGHT OF THE FREE-FLYING HOUSEFLY (*MUSCA DOMESTICA* L.)
I. ORGANIZATION OF THE FLIGHT MOTOR

By H. WAGNER†
Max-Planck-Institut für biologische Kybernetik, Spemannstrasse 38, *D*-7400 *Tübingen, F.R.G.*

(*Communicated by M. F. Land, F.R.S. – Received* 21 *January* 1985)

CONTENTS

Free-flying houseflies have been filmed simultaneously from two sides. The orientation of the flies' body axes in three-dimensional space can be seen on the films. A method is presented for the reconstruction of the flies' movements in a fly-centred coordinate system, relative to an external coordinate system and relative to the airstream. The flies are regarded as three-dimensionally rigid bodies. They move with respect to the six degrees of freedom they thus possess. The analysis of the organization of the flight

† Present address: California Institute of Technology. Division of Biology 216–76, Pasadena, California 91125, U.S.A.

 [Published 25 July 1986

motor from the kinematic data leads to the following conclusions: the sideways movements can, at least qualitatively, be explained by taking into account the sideways forces resulting from rolling the body about the long axis and the influence of inertia. Thus, the force vector generated by the flight motor is most probably located in the fly's midsagittal plane. The direction of this vector can be varied by the fly in a restricted range only. In contrast, the direction of the torque vector can be freely adjusted by the fly. No coupling between the motor force and the torques is indicated. Changes of flight direction may be explained by changes in the orientation of the body axes: straight flight at an angle of sideslip differing from zero is due to rolling. Sideways motion during the banked turns as well as the decrease of translation velocity observed in curves are a consequence of the inertial forces and rolling. The results are discussed with reference to studies about the aerodynamic performance of insects and the constraints for aerial pursuit.

1. Introduction

The main principle of active flight in animals is flapping the wings. The motion of the wings is controlled by a neural network. This circuitry and the muscle systems connected to it are here called the 'flight motor'. During active flight the motor has to accomplish two tasks: (i) to keep the animal flying by the generation of forces which compensate for gravity and air friction; and (ii) to use sensory information for flight control. This may have been the main reason why in biology two approaches to the study of flight behaviour have developed: the 'aerodynamic approach' providing data on the generation of aerodynamic forces (for reviews about insect flight see Rainey 1976; Nachtigall 1983) and the 'guidance approach', with visual control of flight being an important part (for review in insects see Wehner 1981). Only recently, the significance of the sensory feedback for the maintenance of flight itself has been emphasized (Wendler 1978; Heide 1979; see also Nachtigall 1983). To understand the complex behaviour of a fly during an aerial pursuit, it is necessary to study both the organization of the flight motor and the sensory control systems involved in the visually guided behaviour.

In this study data on free-flying houseflies (*Musca domestica* L.) derived from movie films, are presented. To a first approximation, a fly moving through the air can be regarded as a three-dimensional rigid body. The orientation of such a body in three-dimensional space is given by three angles (Euler angles), which denote the inclination of the three orthogonal body axes (long, transverse and vertical axis). There are three degrees of freedom to translate and three degrees to rotate the body. The movement in these six degrees of freedom is generated by the flight motor and influenced by the aerodynamic properties of the flies as well as by gravity. Thus, one of the goals of this study is to unravel whether the flight motor of houseflies can generate forces and torques in all six degrees of freedom and whether it can do this independently in each of them.

These questions have been tackled in many reports on different insect species and on different degrees of freedom: (for example, locusts (Weis-Fogh & Jensen 1956); *Drosophila* (Vogel 1966, 1967; Götz 1968, 1983; David 1978, 1984; Weis-Fogh 1973); *Musca* (Spüler & Heide 1978; Götz & Wandel 1984); calliphorid flies (Nachtigall 1966, 1979; Blondeau 1981; Nachtigall & Roth 1983). Ellington (1984) performed an exhaustive analysis of hovering flight in insects. However, the entire organization of the flight motor is not yet well understood, even in a single species. The same argument holds for the visual control of flight to which this study is confined. Visual control of movements about the vertical axis as well as the control of lift has been

PHILOSOPHICAL TRANSACTIONS OF THE ROYAL SOCIETY B BIOLOGICAL SCIENCES

thoroughly investigated in tethered houseflies (Reichardt & Poggio 1976; Wehrhahn & Reichardt 1975). In addition, the free flight behaviour of hoverflies has been extensively studied (Collett & Land 1975*a*, *b*, 1978; Collett 1980*a*, *b*). Wehrhahn *et al.* (1982) investigated flight trajectories of houseflies and Zeil (1983) those of marchflies. A three-dimensional study combining both the visual control of flight as well as the underlying organization of the flight motor is still lacking.

The main reasons seem to be: (i) in tethered flight movements in only a restricted number of degrees of freedom can be recorded. Although Blondeau (1981) has published experiments in which he simultaneously measured all forces and torques, his interpretations are not convincing (see Discussion). (ii) Motor outputs are forces and torques. These dynamic variables cannot be measured directly from films. Only the position and the orientation of the body is available. Frame by frame analysis allows the derivation of velocities and accelerations, which are kinematic variables. The relation between kinematics and dynamics is complex in freely moving animals. For example, the influence of inertia during free flight is not yet well understood. (iii) Owing to the wide radius of action of the flies compared with their physical size, the resolution of the animals on the films is poor. Therefore, most studies were based on data obtained from a projection of the environment on a horizontal plane only (Land & Collett 1974; Collett & Land 1975*a*, *b*, 1978; Collett 1980*a*, *b*). Previously, in three-dimensional free flight studies of houseflies, the coordinates of only one point per frame and fly could be reliably determined. Thus, merely the movement of the centre of gravity of the flies could be reconstructed (Wehrhahn *et al.* 1982). Zeil (1983) recorded body orientation of marchflies in the horizontal plane but not in the vertical plane.

In contrast, this study includes (i) the orientation of the body axes in three-dimensional space; (ii) the sideways movements; and (iii) the roll movements of the flies. Therefore, it is the basis for a new analysis of the free flight behaviour in houseflies. In a separate report photographs and reconstructions of the flies' movements are compared (Wagner & Wehrhahn 1986). The intention of this paper is to derive the basic organization of the flight motor. These findings will be discussed with reference to the two approaches of studying flight behaviour mentioned previously. A report on visual control of flight will be given in paper II.

2. Methods

The data analysed in this paper are based on the evaluation of 16 mm and 35 mm movie films. Female and male specimens of *Musca domestica* 5–20 days old, from the institute stock were filmed in cages indoors under artificial illumination (Phillips TL 20 W/86 bulbs driven at 25 kHz) at a mean luminance of about 750 cd m^{-2}. Several fly cages were used. The biggest was 0.9 by 0.9 by 0.9 m and a middle-sized one was 0.4 by 0.4 by 0.4 m. There seemed to be no influence of the size of the cage on the basic flight performance. The temperature in the cages varied between 25 and 29 °C. The flies were briefly anaesthetized with CO_2 to separate males and females. If not stated otherwise, only one sex was filmed at a time: 16 mm films (Kodad VNF) were shot with a high-speed camera (Locam 51-0002) at 100 frames per second. The exposure time was in the range 0.5–2.0 ms to reduce motion blur.

Figure 1 shows a drawing of the apparatus, which has been described elsewhere (Wagner 1980). Two perpendicular two-dimensional projections of the three-dimensional environment could be simultaneously recorded with the aid of a mirror (inset in figure 1; Bülthoff *et al.* 1980).

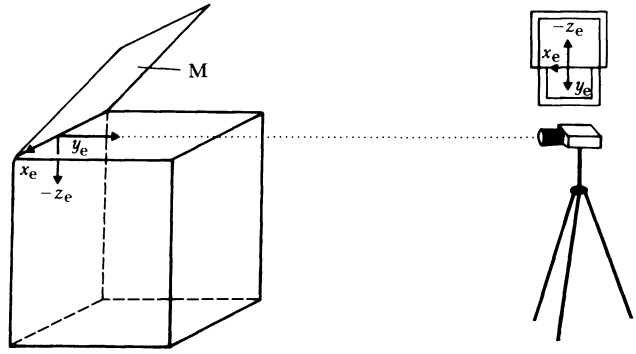

FIGURE 1. The apparatus used for filming. The mirror (M) is mounted at an angle of 45° to the horizontal plane. The camera is positioned at a distance of 4.2 m from the posterior vertical plane of the cage. It is horizontally aligned so that the film plane is parallel to the front of the cage. The walls consist of translucent Perspex. The two walls used for filming are made of normal glass. Lamps are mounted behind the Perspex walls (not shown). The inset shows the scene projected on to the film plane. The upper part denotes the vertical (x_e–z_e) plane, the lower part the horizontal (x_e–y_e) plane as seen from the cage. The inset's edge points below and above the middle point of the midline are the positions of the reference coordinates for the reconstruction of the scene.

In principle, the same method can be adapted to slightly different apparatuses, which were also used: that is, mirror below the cage or on the side. K. Hirschel and C. Wehrhahn shot the 35 mm films with an Arriflex 35BL camera. They synchronized the camera with a high-energy stroboscope (temperature 5400 K) at a frequency of 75 flashes per second. Their fly cage had a size of 23 by 28 by 28 cm. Their film material was Kodak Technical Pan 2415. Parts of these films have been analysed in this study too.

The films were projected on to a digitizing table (Summagraphics-ID) by means of a film projector (Vanguard M 16C-1200-CW-MW, 16 mm films) or a slide projector (Leitz Prado universal, 35 mm films). The position of the fly's head, abdomen and left and right wing base (only in the case of the 35 mm films) were recorded together with a reference point system. To reduce digitizing errors a single frame was digitized up to eight times. After the determination of the mean value the data were stored in a computer (PDP 11/34). In addition, the computer software used for digitizing has been designed to detect errors due to inaccurate digitizing and projection (rotational and translational drift from frame to frame). Thus any point can be recorded with an accuracy of 0.15 mm (twofold standard deviation of the digitizing errors), which is equal to about $\pm 1.25°$ error in the orientation of the long axis at a fly length of 7 mm. In two successive frames a stationary point can be determined within 0.3 mm. Rotational drift between successive frames is negligible. A further means to reduce digitizing errors is a binomial filter of order three:

$$y(t) = 0.25\ x(t-\Delta t) + 0.5\ x(t) + 0.25\ x(t+\Delta t),$$

where x is the input signal, t is time, Δt the time interval between two frames and y is the output signal.

Three-dimensional coordinates of any point in space are computed from the two two-dimensional projections relative to a fixed, right-handed and earth-related coordinate system (figure 2: x_e, y_e, z_e). After this calculation, the data can be transformed to other coordinate systems.

The first step shifts the origin into the thorax of the fly and, thus, leads to x, y, z coordinates.

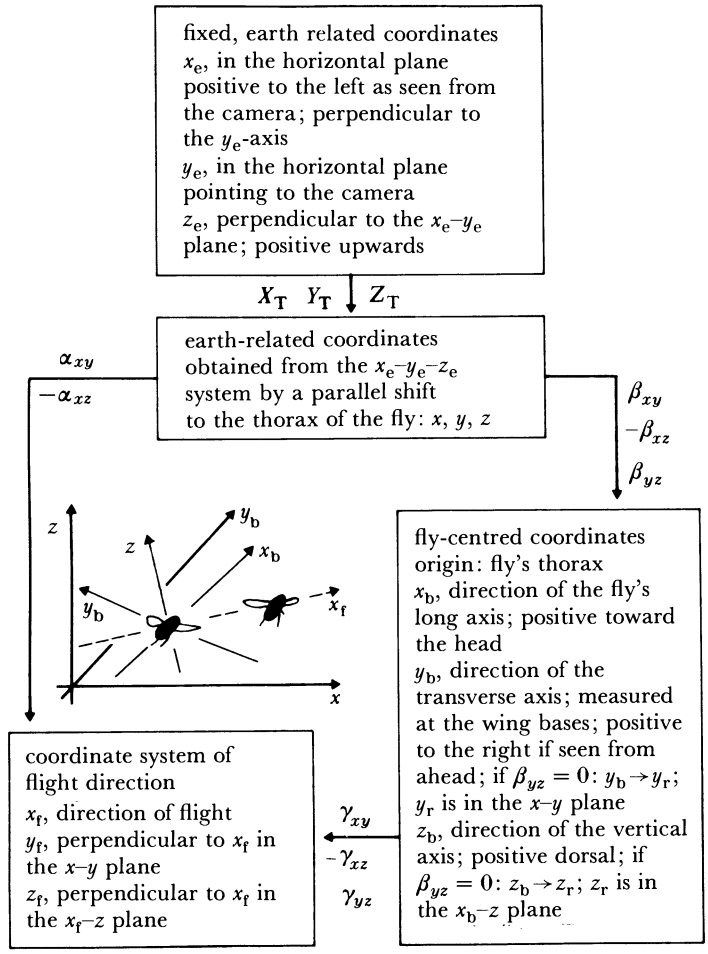

FIGURE 2. Coordinate systems used for the evaluation. The direction of the axes and the Euler angles are denoted. The inset shows a schematic drawing of important axes. X_T, Y_T, Z_T are the values of the fly's thorax position in x_e, y_e, z_e coordinates. In the 16 mm films roll angle could not be measured and is assumed to be zero. Thus, x_r, y_r and z_r axes result. The angles with the index xz have a negative sign, because they represent the Euler angles (see Appendix 1). For further description see text and table 1.

Fly axes (x_b, y_b, z_b or x_r, y_r, z_r, respectively) and flight direction (x_f, y_f, z_f) establish other important coordinate systems. All these coordinate systems are defined as cartesian and right-handed, therefore the coordinate systems can be transformed into each other by the formalism introduced by Euler (see Fifer 1961). Three angles characterize the angular orientation of one coordinate system with respect to another one. The derivation of the angles and the mathematics of the transformation are described in Appendix 1. The angular orientation of the fly axes system (x_b, y_b, x_b) with respect to the x, y, z system is characterized by heading angle β_{xy}, pitch (body) angle β_{xz} and roll angle β_{yz}. The roll angle is not measurable in the x_r, y_r, x_r system. It is assumed to be zero. As a consequence, the y_r axis remains in the x–y plane. In the same manner the orientation of the flight direction system (x_f, y_f, x_f) relative to the x, y, z, system is given by two angles: the horizontal angle of flight direction α_{xy} and the vertical angle of flight direction (ascent angle) α_{xz}. The orientation of the body-axes system to the x_f, y_f, x_f system is given by the angle of sideslip γ_{xy}, the angle of attack (body) γ_{xz} and the angle γ_{yz} due to rolling.

Table 1. List of variables

variables characterizing the movement of the centre of gravity

Δt	sampling time
V_{3D}	three-dimensional translation velocity; the distance travelled between two successive frames divided by the sampling time
v_x	component of V_{3D} in x direction
v_y	component of V_{3D} in y direction
v_z	component of V_{3D} in z direction
V_{xy}	horizontal flight velocity, $\sqrt{(v_x^2+v_y^2)}$
α_{xy}	horizontal flight direction measured in the x–y plane as arctan (v_y, v_x)†; defined from -180 to $+180°$
α_{xz}	vertical flight direction (ascent angle) measured in the x_f–z plane as arctan $[v_z, \sqrt{(v_x^2+v_y^2)}]$†; defined from -90 to $+90°$; as used here, it is the negative value of the corresponding Euler angle
$\dot{\alpha}_{xy}$	change of flight direction in the x–y plane measured as the difference of two successive horizontal flight directions divided by the sampling time

variables that characterize the movement in coordinates centred on the fly's body axes

β_{xy}	heading angle, see Appendix 1
β_{xz}	pitch (body) angle, which is defined here as the negative value of the corresponding Euler angle; see Appendix 1
β_{yz}	roll angle, see Appendix 1
v_f	forward velocity; the distance travelled in the direction of the x_b axis; positive in the direction of this axis; equal to x_b value at time $t+\Delta t$ divided by the sampling time
v_s	sideways velocity; measured according to v_f in the direction of the y_b or y_r axis, respectively
v_u	upward velocity; measured according to v_f in the direction of the z_b or z_r axis, respectively
$\dot{\alpha}_l$	angular velocity about the long axis; measured in x_b, y_b, z_b coordinates as the roll angle of the fly at $t+\Delta t$ divided by the sampling time
$\dot{\alpha}_t$	angular velocity about the transverse axis; measured in x_b, y_b, z_b or x_r, y_r, z_r, coordinates, respectively as the negative pitch (body) angle of the fly at $t+\Delta t$ divided by the sampling time
$\dot{\alpha}_v$	angular velocity about the vertical axis; measured as the heading angle of the fly at time $t+\Delta t$ divided by the sampling time
γ_{xy}	horizontal angle between the direction of the long axis and the flight direction (angle of sideslip); measured as arctan (v_s, v_f)†; defined from -180 to $+180°$
γ_{xz}	vertical angle between the direction of the long axis and flight direction (angle of attack (body)) measured as arctan $[v_u, \sqrt{(v_s^2+v_f^2)}]$†; defined from -90 to $+90°$; it is the negative value of the corresponding Euler angle
γ_{yz}	angle between flight direction and body axes coordinate system due to rolling

† Arctan (y, x) is a computer program that calculates the arc of the tangent from -180 to $+180°$.

In table 1 these and further variables are specified. As kinematically relevant variables the velocities and accelerations give insight into the flight performance and organization of the flight motor. Three-dimensional translation and angular velocity as well as the force and the torque define a vector. Since the flight motor is body-centred, the vector components related to the body axes are considered. The components of the torque vector in the direction of the vertical, transverse and long axis are yaw, pitch and roll, respectively. In the same manner, the force vector components are upward thrust, sidethrust and forward thrust. The component of the force vector operating against gravity is lift and the component in the horizontal plane is thrust. Drag is a frictional force that acts against the direction of flight.

If not stated otherwise, only data on females are presented in this paper. I try to derive properties of the flight motor from 'cruising flights' (Collett & Land 1975*a*). About 1700 frames at a time interval of 10 ms have been digitized from 16 mm films. On these films, flies appear as cylinders. Therefore, two points (one on the head (circle), the other on the abdomen (end point of the line indicates the long axis)) indicate the position and the flight posture of the flies in the 16 mm films (figures 4, 7 and 8). With this method the heading angle β_{xy}, the pitch (body) angle β_{xz} and forward velocity v_f, as well as all parameters defining the flight trajectory

(V_{3D}, v_x, v_y, v_z, α_{xy}, α_{xz}, $\dot{\alpha}_{xy}$ and derivatives) can, in principle, be measured exactly. A complete reconstruction of the angular orientation of the fly axes could be obtained from the 35 mm films. The inclination of the transverse axis is indicated by the triangle in figure 3*a*. 500 frames, at a time interval of 13.33 ms, have been analysed from these films.

3. Results

3.1. *Three-dimensional flight performance*

Figure 3*a* shows a stereopair of a cruising flight viewed from above. Looking at the flight track through stereoglasses reveals the fly's excursions in the third (vertical) dimension. The fly rotates about each of the three body axes (figure 3*h–k*) and performs translatory movements in the direction of these axes (figure 3*b–d*).

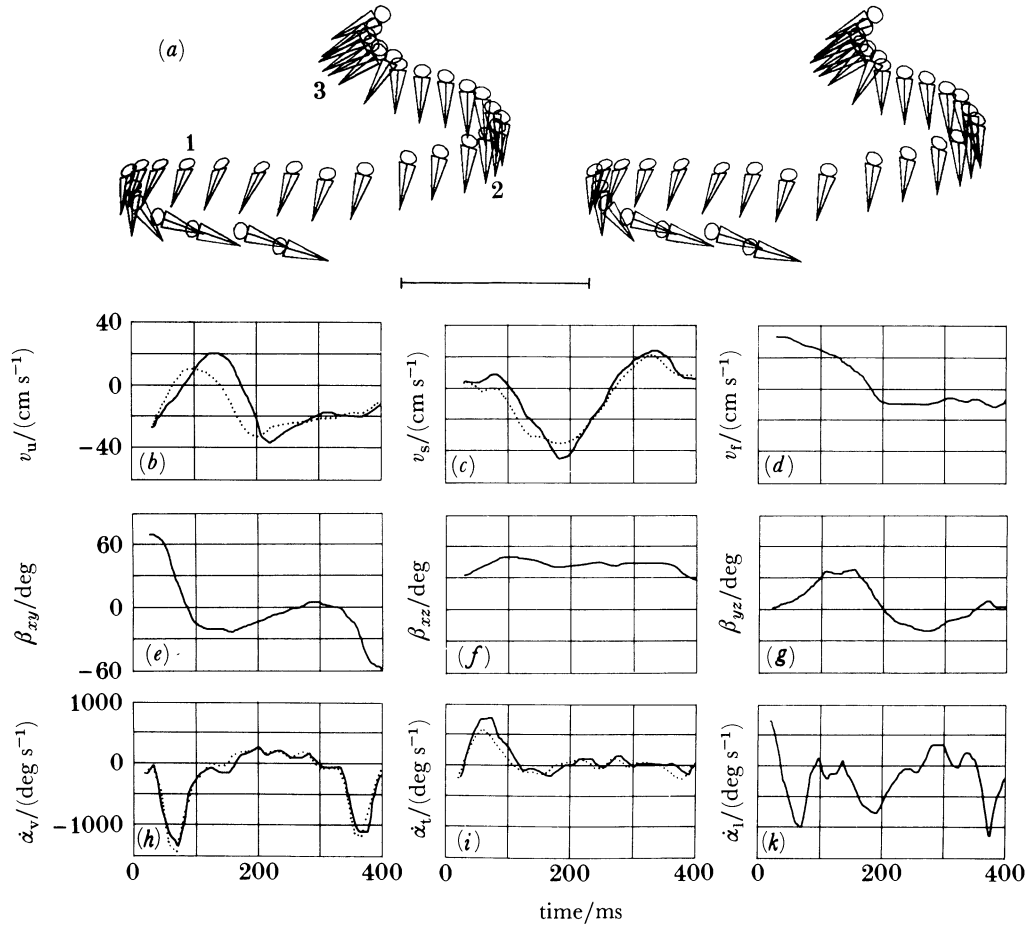

Figure 3. Cruising flight reconstructed from a 35 mm film. The circle gives the position of the fly's head; the line the direction of its long axis. The triangle represents the connection of the wing bases to the head and the abdomen. Successive drawings denote the position in successive frames. The time interval is 13.33 ms. Every tenth frame is numbered. The scene is viewed from above. If lens stereoglasses are used, excursions in the third (vertical) dimension can be seen. Marker: 2.5 cm; (*b*)–(*k*) time plots of variables, filtered values. (*b*) Upward velocity v_u; (*c*) sideways velocity v_s; (*d*) forward velocity v_f; (*e*) heading angle β_{xy}; (*f*) pitch (body) angle β_{xz}; (*g*) roll angle β_{yz}; (*h*) angular velocity about the vertical axis $\dot{\alpha}_v$; (*i*) angular velocity about the transverse axis $\dot{\alpha}_t$; (*k*) angular velocity about the long axis $\dot{\alpha}_l$. The dotted lines in (*b*), (*c*), (*h*) and (*i*) give the values of the variables if zero roll angle is assumed. A movement in all six degrees of freedom is found. Rotational movements are not coupled to each other, because the different changes of the flight direction underly different patterns of angular movements (*h*)–(*k*).

The first turn in the example of figure 3*a* (40–120 ms) consists of a rotation about all three axes. This turn is banked: the fly lowers the side pointing into the centre of the curve as an aeroplane does in a curve. After completing the turn the fly moves nearly perpendicularly to its long axis (120–320 ms). During this period the roll angle changes sign while the fly sinks down and falls back (figure 3*d*, *g*). The fly then performs a change of flight direction by a slight change in long-axis orientation only (figure 3*e*, *g* at about 250 ms). The final turn is characterized by a rotation about the vertical and long axis (figure 3*h*–*k*). All movements are performed head up at a pitch (body) angle well above zero (figure 3*f*). The time course of the translation velocities (*b*–*d*) is much smoother than that of the angular velocities. The latter appear to change in discrete steps with a steep rise and fall (figure 3*h*–*k*, and especially figure 4*e*). Figure 4 shows an example of much longer duration.

The time course of the angle of sideslip (figure 4*b*) indicates that the fly's long axis is seldom exactly aligned with the direction of flight. Furthermore, the time course of the angle of attack

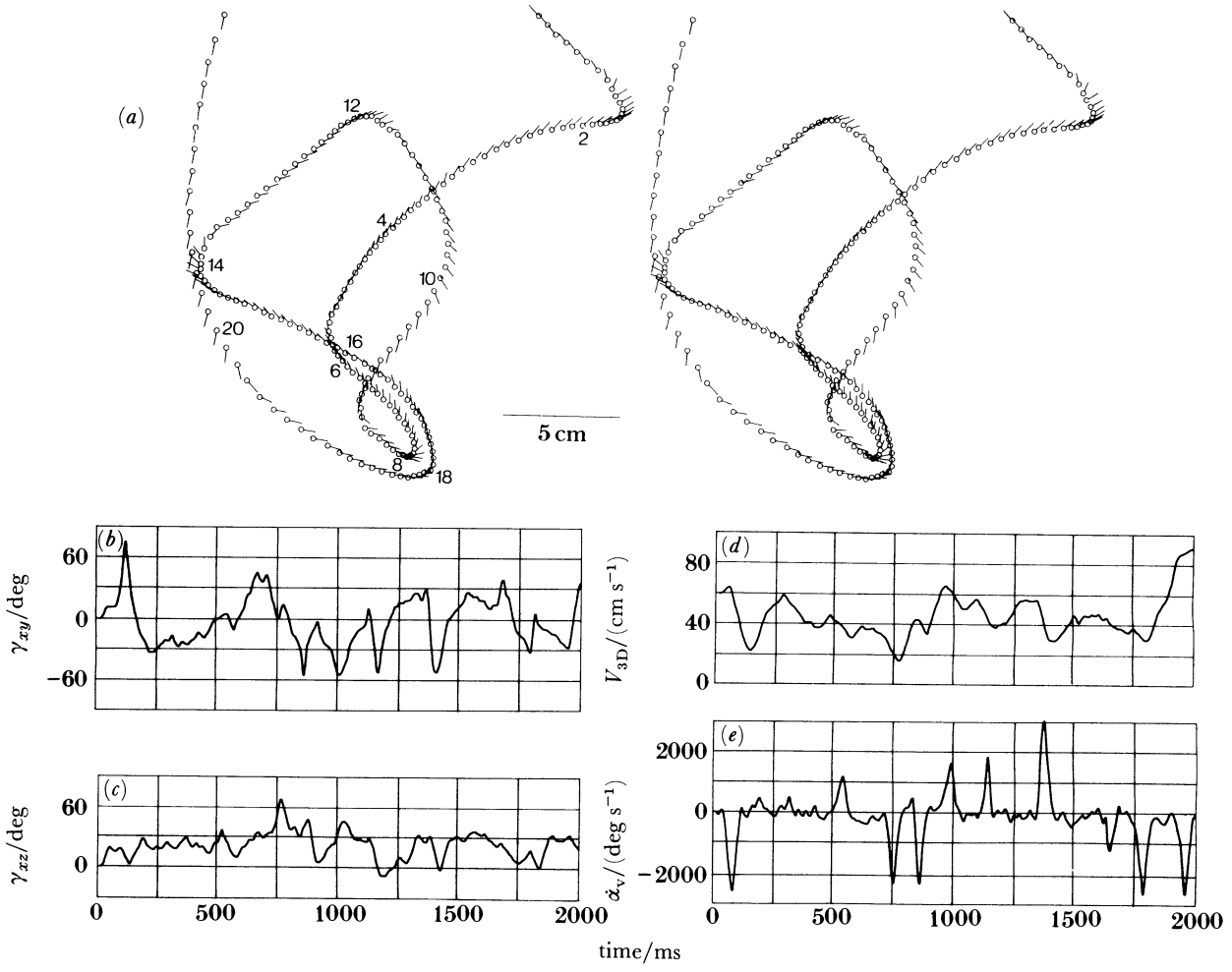

FIGURE 4. Cruising flight reconstructed from a 16 mm film. (*a*) Trajectory. Notation as in figure 3. The time interval is 10 ms. Numbers refer to 0.1 s. (*b*)–(*e*) Time plots of variables (0–2 s), filtered values. (*b*) Angle of sideslip γ_{xy}; (*c*) angle of attack (body) γ_{xz}; (*d*) three-dimensional translation velocity V_{3D}; (*e*) angular velocity about the vertical axis $\dot{\alpha}_v$. Angular movements are characterized by periods of only little or no turning interrupted by large changes of axis orientation (*a*), (*e*).

(figure 4*c*) shows that the body is inclined to the flight direction so that the air strikes it from below. These two characteristics might be in part a consequence of the experimental situation (that is, the small cage). Different body movements may lead to similar flight paths. During the almost straight flight paths in figure 4*a* (0–0.1 s, 1.2–1.4 s) and figure 3 (120–320 ms), for example, the angle of sideslip is different. Flight direction changes more than body direction during the first turn in both figure 3*a* and figure 4*a*. Thus a reconstruction of the flight trajectory, showing only the movement of the fly's centre of gravity, does not reveal most of the movements of the fly's body.

The first example (figure 3) is reconstructed from a 35 mm film, the second (figure 4) from a 16 mm film. In the second example the roll angle could not be measured and has been assumed to be zero. Since roll angles of up to 90° have been observed, errors in the evaluation of the data in the 16 mm films will occur. To estimate these errors, the data of the 35 mm films have been evaluated in two different ways (figure 3*b*, *c*, *h*, *i*): (i) considering the roll angle (solid lines) and (ii) assuming zero roll angle (dotted lines; equal to the situation in the 16 mm sample). A roll angle different from zero affects translational and rotational variables related to the transverse and vertical axis. At a roll angle of 90°, for example, the body axes are interchanged: the y_b-axis is oriented in the direction of the z_r-axis. The effect of neglecting the influence of the roll component on to the other variables consists, however, mainly of a reduction of amplitude rather than a change in the time-dependent behaviour. Therefore, the quite good correspondence observed in figure 3*b*, *c*, *h*, *i* is not surprising.

The linear cross-correlation coefficients between corresponding pairs of (i) angular velocities about the z_b or z_r axis, respectively (vertical angular velocities), (ii) the corresponding pairs of angular velocities about the transverse axis, (iii) sideways velocities and (iv) upward velocities lie between 0.9 and 0.95. The slopes do not differ from 1. Thus it can be stated that the errors made if the roll angle cannot be measured, as in the 16 mm films, should not critically influence the conclusions drawn from the evaluation but mainly increase the scatter in the average data samples. In single examples the effect of rolling can be related to parameters measurable from the 16 mm films (3.2.3, Appendix 2). It should be mentioned that, during banked turns, often a change of the sign of the angular velocity about the transverse axis is observed when zero roll angle is assumed which is not found if the roll angle is considered.

3.2. *How are the movements generated?*

Although movements of the flies with respect to all six degrees of freedom are found, this does not necessarily mean that the flight motor generates torques and forces in all degrees of freedom. Gravitation is an external force that influences flight. In addition, frictional and inertial forces and torques are generated by motion. The sum of the forces can be formally denoted as

$$\boldsymbol{F} = \boldsymbol{F}_A + \boldsymbol{F}_G + \boldsymbol{F}_M, \tag{1}$$

where $\boldsymbol{F}$, the accelerating forces, are equated with frictional forces $\boldsymbol{F}_A$, gravitational forces $\boldsymbol{F}_G$ and motor forces $\boldsymbol{F}_M$. Similar equations apply for the torques. Since the aerodynamic friction coefficients as well as the exact position of the centre of gravity are not known, the exact action of the flight motor cannot be derived. However, to study the principal organization of the flight motor, quantitative values of the forces and torques are not necessary. It is argued here that the basic organization can be outlined from (i) the rotational behaviour of the flies due to the

PHILOSOPHICAL TRANSACTIONS OF THE ROYAL SOCIETY B BIOLOGICAL SCIENCES

'steplike' changes of orientation of the body axes (figure 3*h–k*, figure 4*e*); (ii) the dependence of the vertical and horizontal translational movement on the pitch (body) angle and (iii) the relation between the sideways movements, the roll angle and the inertial (ballistic) forces.

3.2.1. *Angular velocities and torques*

For a substantial part of the time the values of the angular velocities are small and masked by the digitizing errors so that the angular orientation of the body remains nearly constant. These periods are interrupted by sudden changes in body orientation accompanied by peaks of the angular velocities. These events are called 'turns'. A turn starts from a value of the angular velocity of about zero. At the end, a zero value is attained once more (see figure 4*e*). Thus, the time course of the angular velocities may be characterized by a series of peaks separated by periods of little or no turning. A significant dependence of angular velocities on aerodynamic parameters (angle of attack (body), angle of sideslip) has not been observed. Therefore, the peaks of the angular velocities indicate the generation of significant torques. Simultaneous peaks were expected, if the generation of the torques about the different axes were coupled. Thus, the temporal distribution of the peaks measured with respect to the different axes allows one to deduce the coupling of the torques.

Digitizing errors for the angular orientation lie in a range of $\pm 1.5°$. At 75 frames per second this means an error in angular velocity of about $\pm 225°$ per second. All velocity values outside this range are regarded as values representing a 'true' change of axis orientation. A turn may be characterized by the time it lasts and the change of axis orientation to which it leads. Consecutive values above threshold value are summed to give the turning amplitude (α_V). Turning time (t) is defined as time between exceeding threshold value and falling below this value again. During a single turn about the long axis, but not during turns about the other axes, the sign of the angular velocity may change (figure 3*k*, 120–320 ms). Therefore, a turn was assumed to last from the first value exceeding the threshold to the next but one falling below the threshold in such cases. With this method of evaluation changes of body orientation of long duration and at subthreshold angular velocity cannot be registered. However, such movements seem not to be present (paper III) and they are not critical for the arguments here. In addition, as only the presence of a turn has to be detected, but not its exact time course and turning amplitude, it is not critical that, with this method, errors are accumulated.

Table 2 documents the turns found by this method of evaluation. There is a clear tendency towards a simultaneous occurrence of angular velocities about at least two axes (42 out of 59 cases). However, a movement about a single axis, without a movement about the other ones, is observed for each of the axes. This is a strong indication that the torques about the axes can be generated independently. Since for both the rotation about the vertical and the transverse axis only one example has been observed, this conclusion needs further support: (i) There is no strict coupling of the direction of the simultaneous rotations about the different axes; already the few data of table 2 reveal many combinations of directions. (ii) The temporal coordination during simultaneous modulation of angular velocities varies (table 3); roll movements, for example, often start before, and/or end after, angular movements about the other two axes. Thus the flight motor of *Musca* can generate movements about the body axes independently of each other. In other words, the vector composed of the three angular velocities and accelerations is not at all fixed with respect to the body axes.

Despite this principal independence some characteristic combinations are more likely to

TABLE 2. OCCURRENCE OF TURNING: DISTRIBUTION OF THE TURNS ABOUT THE DIFFERENT AXES

		vertical axis								
		0			+			—		
		transverse axis								
		0	+	−	0	+	−	0	+	−
long axis	0	·	1		1	1	·	·	·	·
	+	15	·	1	·	1	·	1	·	·
	−		·	2	1	·	·	5	2	1
	+/−	·	·	·	1	·	·	2†	9†	2
	−/+	·	1	·	2†	6†	2	2		

Turning amplitudes are used for the characterization of the angular movements; threshold values, ±1.5° of change of axis' orientation.

Total number, 59.

Symbols, 0, +, −, +/−, −/+ give the direction of rotation and temporal changes of this direction.

† Banked turns.

TABLE 3. TEMPORAL COORDINATION OF TURNING: DISTRIBUTION OF ONSET AND STOP OF THE TURNS, WHEN THE MOVEMENT ABOUT THE DIFFERENT AXES IS COMPARED

time interval (×13.33 ms)	vertical and long axis (vertical leading) +		vertical and transverse axis (vertical leading) +		transverse and long axis (transverse leading) +	
	onset	stop	onset	stop	onset	stop
−5	1	2	0	0	0	0
−4	0	1	0	0	2	1
−3	3	4	0	0	1	0
−2	2	3	0	1	4	4
−1	8	5	1	3	5	5
0	6	5	6	5	4	1
1	5	0	9	4	2	3
2	1	0	1	2	1	1

Numbers are not equal for onset and stop of the turns because sometimes the turns started before or ended after the beginning of the evaluation. The numbers give less than the sum of table 2, because a certain combination of rotations can often be detected, however, not when the turn starts or ends. To avoid the complex interrelations between the three rotations only the movement about two axes, irrespective of the movement about the third axis, is considered at one time.

occur. The patterns of banked turns (table 2), similar to the turn shown in figure 3*a*, may serve to maintain aerodynamic stability during curved flight. Frequently the flies perform only roll movements (table 2). By doing this, they are able to fly straight at an angle of sideslip differing from zero.

3.2.2. *Pitch (body) angle and translational movement*

The flight motor generates lift and thrust to counteract gravity and air-friction. The relations between the pitch (body) angle, the ascent angle (related to lift) and the horizontal flight velocity (related to thrust) provide further insight into the organization of the flight motor. If the direction of the force vector could be freely adjusted by the fly, no correlation should be found. If, on the other hand, the force vector had a fixed inclination relative to the body

PHILOSOPHICAL TRANSACTIONS OF THE ROYAL SOCIETY B BIOLOGICAL SCIENCES

axes, ascent angle and horizontal flight velocity should, in case of stationary conditions, depend on pitch (body) angle in a predictable manner:

(i) When the ascent angle reaches 90°, the direction of the force vector is vertical and the horizontal flight velocity (V_{xy}) is zero. Then the difference between ascent angle (α_{xz}) and pitch (body) angle (β_{xz}) gives the inclination of the force vector to the long axis (δ_{xz}).

(ii) Zero ascent angle corresponds to level flight. Under this condition the fly just lifts its own mass ($G \approx 2 \times 10^{-4}$ N).

(iii) Maximum horizontal flight velocity ($V_{xy}(0)$) results if the force vector is directed horizontally. In this situation, pitch (body) angle is $-\delta_{xz}$. If the total force $\boldsymbol{F}_M$ is independent of body inclination, the following theoretical relationship can be derived:

$$\alpha_{xz} = \arctan\left(\frac{\boldsymbol{F}_M \sin(\beta_{xz}+\delta_{xz}) - G}{\boldsymbol{F}_M |\cos(\beta_{xz}+\delta_{xz})|}\right). \tag{2}$$

Notice that (2) is derived from (1) by splitting it up in a vertical and horizontal part. It is further assumed that no acceleration takes place ($\boldsymbol{F} = 0$) and that the contribution of $\boldsymbol{F}_G$ in the horizontal direction is zero. The last assumption is straightforward. The evaluation shows that the first is sufficiently fulfilled too.

There is some debate whether in small insects thrust is proportional to flight velocity or the square of velocity (Vogel 1966; Götz 1968; David 1978; Ellington 1984). My data do not allow a choice between these two possibilities, therefore (3) denotes both dependences. If the mean horizontal velocity is assumed to be proportional to thrust,

$$V_{xy} = V_{xy}(0) |\cos(\beta_{xz}+\delta_{xz})|, \tag{3a}$$

or if the mean horizontal velocity is proportional to the square root of thrust,

$$V_{xy} = V_{xy}(0) \sqrt{|\cos(\beta_{xz}+\delta_{xz})|}. \tag{3b}$$

In figure 5*a* the relation between pitch (body) angle and the ascent angle as well as horizontal flight velocity are shown. Similar dependences are found also in chasing and non-chasing males

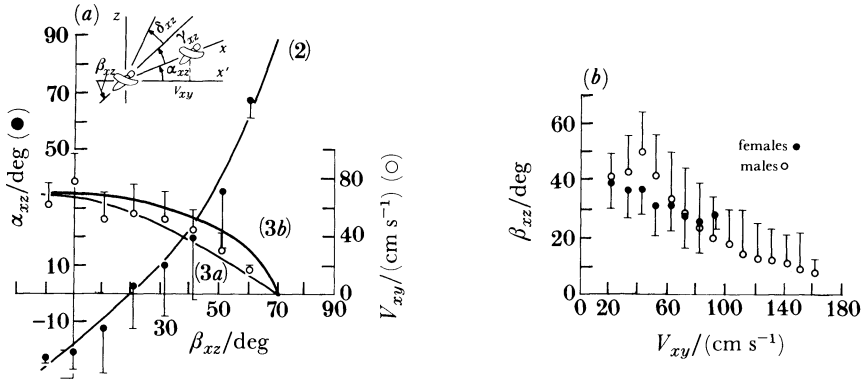

FIGURE 5. The influence of pitch (body) angle on translational movement; (*a*) the dependence of ascent angle α_{xz} and the horizontal flight velocity V_{xy} on pitch (body) angle β_{xz} (see inset). The abscissa is divided into bins of 10° width. All the values falling into one bin are averaged and shown with the standard deviation. Mean ascent angle (●) depends on pitch (body) angle. Horizontal flight velocity (○) depends in a reverse manner on pitch (body) angle as ascent angle. Lines represent the theoretical curves under the assumption that the direction of the force vector is fixed to the body and the total force is independent of pitch (body) angle (see text). (*b*) At level flight a dependence between horizontal flight velocity V_{xy} and pitch (body) angle β_{xz} is found. Filtered values are plotted.

as well as in tracking females. Only values of the pitch (body) angle with a corresponding angle of sideslip of less than $\pm 10°$ are considered because these values most closely represent forward flight. The abscissa is divided into bins of 10° width and the values of the ascent angles falling within one bin are averaged to approximate stationary conditions. The same is done for the horizontal flight velocity. The mean values and standard deviations are displayed. Implicitly it is assumed by this method of evaluation that the ascent angle shows the vertical force components. This seems to be justified because the mean change of the ascent angle does not differ much from zero for all bins of pitch (body) angles. The mean horizontal acceleration is small too, but it has a gradient from -260 to $+100$ cm s^{-2} over the range of pitch (body) angles found here. Calculations show that the accelerating forces thus generated do not critically influence the graphs of (2) and (3), which are represented by the lines of figure 5*a*. Therefore it is concluded that the conditions underlying the evaluation are a sufficient approximation to stationary conditions and the above equations can be used.

The parameters of these curves are as follows:

(i) Extrapolation leads to an ascent angle of 90° at a pitch (body) angle of about 70° (range of error about $\pm 5°$); thus δ_{xz} amounts to about 20°.

(ii) Zero ascent angle corresponds to a pitch (body) angle of about 20°. Equation (2) then reduces to

$$0 = \boldsymbol{F}_{\mathrm{M}} \sin(\beta_{xz} + \delta_{xz}) - G \tag{4}$$

with

$$\boldsymbol{F}_{\mathrm{M}} = \frac{G}{\sin(\beta_{xz} + \delta_{xz})} \approx \frac{20}{0.64} \times 10^{-5}\ \mathrm{N} \approx 31 \times 10^{-5}\ \mathrm{N}. \tag{5}$$

(iii) The maximum of the mean horizontal flight velocity $V_{xy}(0)$ amounts to *ca.* 70 cm s^{-1}. The three-dimensional flight velocity declines with increasing pitch (body) angle (not shown). However, a decrease is expected because of the action of gravity, if the total force remains constant.

The theoretical curves correspond well with the data. Thus it can be stated that the dependence of the mean ascent angle as well as the mean horizontal flight velocity on the pitch (body) angle is consistent with the hypothesis that the direction of the force vector is fixed relative to the fly's long axis. If this conclusion were correct, at different translation velocities different body inclinations should occur at a given flight direction. For level flight the mean pitch (body) angle decreases with increasing horizontal velocity (figure 5*b*). The effect is not pronounced in females. It can be clearly seen only if the data of males that fly at higher velocities are included in the diagram. Additional observations that are not documented reveal that the mean angle of attack (body) amounts to about 20°. This angle is found to be independent of body inclination for pitch (body) angles between -10 and $+40°$. The angle of attack (body) decreases with increasing ascent angle. Houseflies do not actively fly backwards.

From these mean values a very simple flight behaviour would be expected: at a given pitch (body) angle and flight velocity the fly should be able to fly in one (vertical) direction only. However, there are indications that the flight performance is more complex. For example, males may climb at ascent angles of 80–90° with a nearly vertically inclined long axis. This is possible only if the direction of the force vector does not deviate much from the direction of the long axis. In some of the examples the ascent angle increases at constant flight velocity. These examples indicate some variability in the direction of the force vector (see also Discussion).

PHILOSOPHICAL TRANSACTIONS OF THE ROYAL SOCIETY B BIOLOGICAL SCIENCES

3.2.3. *The source of sideways motion*

An unexpected observation emerging from these films concerns the flies' sideways movements (figures 3, 4 and 8). The forces causing these movements could be a sidethrust produced by the flight motor, inertial (ballistic) forces or gravity. First, gravitational and inertial influences on sideways motion will be examined to test the hypothesis that the flight motor generates no active sidethrust. Thus, the force vector is located in the midsagittal plane. It is assumed to be inclined to the long axis at some positive angle (upward, figure 5).

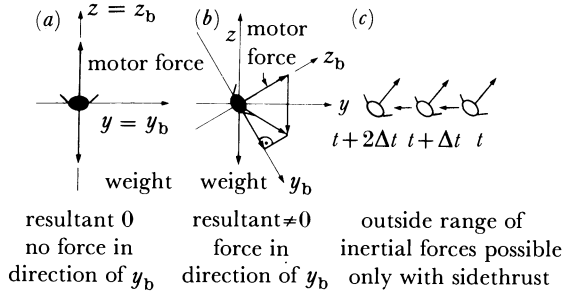

FIGURE 6. In a system with gravity a sideways component is induced if the roll angle is not zero. Horizontally aligned fly seen from front; the upward thrust equals the mass of the fly; (*a*) at zero roll angle level flight results; (*b*) at a roll angle of −60° the induced sideways thrust is considerable; (*c*) outside of range of inertial forces this movement can only be explained by a motor sidethrust; no such example has been found so far. For further explanations see text.

As is explained in figure 6*a* and *b*, gravity causes a sideways force at roll angles differing from zero. Consequently, the sideways acceleration and velocity should depend on the roll angle. In fact, the correlation between the sideways acceleration and the roll angle is strongest if the values at the same instant of time are compared. The linear correlation coefficient amounts to about −0.7 (ten examples of cruising flight). The strongest correlation between the sideways velocity and the roll angle is found if the values of the sideways velocity are delayed by 80 ms with respect to the values of the roll angle (linear cross-correlation coefficient about −0.8). The latter result indicates that inertia plays a role during sideways motion.

Inertial forces are generated in accelerating systems. For flying insects of the size of *Musca* it was assumed that an immediate balance of the drag and the motor force is established, leading to a proportionality between velocities and forces (Poggio & Reichardt 1981; Wehrhahn *et al.* 1982). What is 'immediate'? Turns of *Musca* last some 20–100 ms. A common observation in my examples is that during a turn about the vertical axis the horizontal flight direction does not change at once, but with a delay of up to 100 ms (figures 4*a*, 8*a*). The delayed change of flight direction is interpreted as a consequence of the inertial forces. Indeed, as is expected from this conclusion, the maximum sideways acceleration reached during a turn depends on the three-dimensional flight velocity at the beginning of the turn (linear correlation coefficient 0.77, 26 examples). An alternative interpretation of the observed sideways motion could be that a force in the direction of the transverse axis is generated simultaneously with a torque about the vertical axis by the flight motor. This seems to be very unlikely because only a weak correlation between maximum sideways velocity and angular velocity is found. Moreover, the maximum of the sideways velocity is delayed by 20–30 ms with respect to the maximum of

the angular velocity. This, by itself, indicates inertial effects. Recently, David (1984) has reported influences of inertia on the flight of *Drosophila* too. In addition, I examined the data for an example that qualitatively deviates from the patterns just described. As is indicated by the negative correlation coefficients, the roll angle and the sideways velocity normally have different signs. Thus, if the signs of the roll angle and the sideways velocity would be equal, a movement similar to that indicated in figure 6*c* would result. If such a movement could not be explained by the interial forces acting on the fly it would be a strong indication of an actively generated sidethrust. So far I have not found such an example.

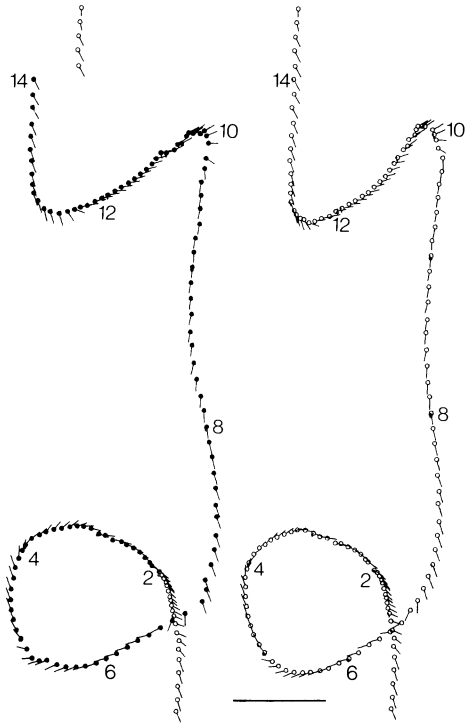

FIGURE 7. Sideways movement can be explained without a sideways force produced by the flight motor. ○, originally reconstructed flight path; ●, flight path, in which the sideways movement, but not the other degrees of freedom were calculated with the algorithm denoted in Appendix 2; start of simulation at frame number 20, end at frame number 140; parameters are given in Appendix 2. Numbers denote the time in 100 ms. Bar denotes 5 cm.

By simulating flights it can be tested whether the influence of the roll angle and the inertial forces are sufficient to explain the observed sideways movements. Figure 7 shows the comparison of a flight trajectory (open symbols) with a simulation (filled symbols). The correspondence is good. The algorithm used for the simulation is explained in Appendix 2. Thus, the sideways movements of *Musca* can be, at least qualitatively, explained without a sidethrust generated by the flight motor.

3.2.4. *Rotations and translations*

The flies' angular movements are not influenced by the three-dimensional translation velocity: turns of similar size and duration can be performed at different translation velocities (figures 4 and 8). This is especially obvious during the pursuit of small targets (paper II).

Similarly, translation is, in principle, not determined by the angular movements of the body (figure 8*b*, *e*). Thus, it seems that the torques and the force of flight can be generated independently of each other.

As described above, flight direction depends in a complex way on the body movements. Knowing the principal organization of the flight motor, one can try to interpret those examples in which only the orientation of the long axis, but not that of the transverse axis, could be recorded. First, the straight flight in figure 4*a* (1.2–1.4 s) at an angle of sideslip of about 20–30° is probably due to rolling of the body and not due to an active sidethrust generated by the flight motor. Secondly, it has been observed here and previously in cruising flights of *Fannia* (Land & Collett 1974) and *Drosophila* (Bülthoff *et al.* 1980) that the translation velocity decreases during sharp changes of the direction of flight. The mechanism underlying this decrease in velocity is not understood so far.

Figure 8*a* shows a flight sequence with two turns (arrows) leading to similar changes of the body direction (figure 8*e*). However, the changes of the three-dimensional translation velocity differ. During the first turn the velocity drops marginally (figure 8*b*, arrow). During the second

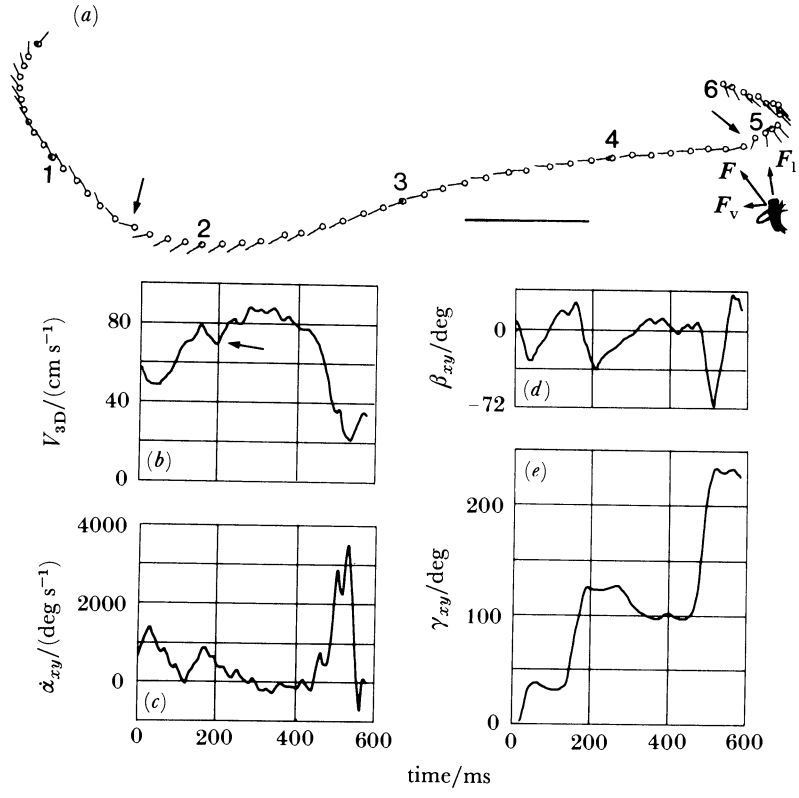

FIGURE 8. The effect of rolling in curves. During the first and the second turn the changes of the orientation of the long axis are similar (arrows and (*e*)). The effect on the trajectory is quite different. It can be seen that during the first turn the angle of sideslip γ_{xy} changes its sign and remains small, whereas during the second turn it reaches a value of more than 70° (*d*). The influence on the translation velocity V_{3D} (*b*) and the change of flight direction $\dot{\alpha}_{xy}$ (*c*) is interpreted with knowledge from the 35 mm data. If the force vector would remain in the midsagittal plane, during the second turn, but not during the first turn a force component against the former flight direction would occur. Inset in (*a*) shows hypothetical orientation of fly's body, wings and legs. The force vector is split up into components in the direction of the long axis $\boldsymbol{F}_l$ and the vertical axis $\boldsymbol{F}_v$. The latter is supposed to be responsible for the deceleration (*b*). In (*b*)–(*e*) the filtered values are plotted. Bar denotes 5 cm. Notice that the trajectory is part of that drawn in figure 7.

turn the velocity decreases sharply. The main differences between the two manoeuvres are: (i) during the second turn the angle of sideslip increases to more than 70°, whereas during the first turn it changes sign and remains less than 35°; (ii) the change of flight direction is much greater during the second than during the first turn. An explanation for this may be that the angle of sideslip is an indicator for the roll angle during straight flight. Thus, before the first turn the roll angle would be negative. It would be zero or positive afterwards. The second turn looks like the banked turn in figure 3*a*, where the vertical axis of the fly pointed into the centre of the curve. During such a turn the force vector of the fly, inclined upwards in the fly's midsagittal plane, has a component directed against the direction of flight before the turn is accomplished (inset in figure 8*a*). Thus, the decrease in the translation velocity can be explained as a consequence of flight motor organization.

4. Discussion

In this study the movements of houseflies have been analysed. The orientation of the fly's body axes in three-dimensional space has been recorded. The determination of the roll movements seems to be not essential for a correct description of the flight manoeuvres because the effect of rolling can be attributed to variables that are measurable from the change in long axis orientation. In contrast, the movement of the centre of gravity does not reveal many aspects of the flight behaviour.

The main results of this study are the following. The flight motor of *Musca* generates a force the direction of which varies much less relative to the body axes than the vector composed of the torques. Sideways movements are not the result of an independent sidethrust but rather of a complex phenomenon influenced by inertia and gravity. Many complicated relationships between the body movements and the changes of flight direction become understandable (§3.2.4.). No differences between females and males have been observed. In addition, the basic flight performance described here seems to be independent of the behavioural situation. Since these conclusions were derived from kinematic and not dynamic measurements, their validity has to be considered in detail.

4.1. *Force vector inclination*

The force vector may be characterized by its inclination to the body axes and its position relative to the centre of gravity. The force vector of houseflies flying stationary in still air is inclined 29° to the long axis (Götz & Wandel 1984). Similarly Vogel (1966), Götz (1968) and David (1978) observed fixed inclinations of the force vector in drosophilid flies. Can this be expected in free flight, too? The angle at which the wings are struck by the air, and thus the direction of the force vector, depends on the geometrical angle of attack (wings) and the flight velocity. A force asymmetry develops with increasing flight velocity as has been nicely demonstrated by Ellington (1984, p. 54). Thus, even in stationary free flight, the force vector inclination would depend on flight velocity and would not be so stable as in fixed flight. However, the force asymmetry depends on the change of the advance ratio (the quotient of flight velocity and flapping velocity). This ratio depends on the flight velocity and therefore on the pitch (body) angle too. Rough calculations show that the advance ratio will be about 0.1 at $\beta_{xz} = 60°$ and not greater than 0.5 at $\beta_{xz} \approx 0°$. According to Ellington's model and under the assumption that the wing stroke plane has a fixed inclination to the long axis, this would

mean that the direction of the force vector would change about 50° at a change of body inclination of about 60° in free flight of *Musca*. This amount does not exceed the variability of the direction of the force vector observed in single cases.

A first-order indicator for the force vector inclination would be hovering flight (David 1978). Unfortunately, *Musca* does not hover. I have inspected more than 2 h of flight tracks of *Musca* on films and have found only one sequence in which the fly tended to stand still in the air (duration about 100 ms). Therefore, the averaged kinematic data presented in figure 5 and the inspection of single examples are the only basis of the interpretation. It seems that the direction of the force vector can be varied around a mean value of about 20° within a limited range only. Similar conclusions have been drawn by Blondeau (1981) and Nachtigall & Roth (1983) for calliphorid flies. Thus, muscid, drosophilid and calliphorid flies behave in a similar way with respect to the generation of lift and thrust.

These findings imply that the flies generate much greater thrust forces than measured in wind tunnels (Weis-Fogh 1956; Vogel 1966). This discrepancy cannot be solved here and no speculations will be made about the possible reasons. Experiments in which the thrust can be directly measured and related to flight speed are necessary in the future.

It is intriguing to find a similar dependence of the ascent angle on the inclination of the body in free-flying houseflies and locusts (Baker *et al.* 1981). The relation between the ascent angle and the angle of attack is also similar to these two species. Interestingly, locusts have been reported to be able to control lift independently of thrust (lift-control reaction, Gettrup & Wilson 1964). It has been assumed that the flight behaviour of small insects differs from that of locusts in that they cannot control lift independently of thrust (Vogel 1966). In free-flying houseflies some variability of the direction of the force vector has been observed. If the lift-control reaction in locusts were also to be restricted to a certain range (Gettrup & Wilson tested only pitch (body) angles between 0° and 30°) or if it played only a minor role in free flight, the similarity of the flight behaviour in muscid flies and locusts would not be surprising. Esch *et al.* (1975) describe a similar relationship as that shown in figure 5 for flying bees.

Since the mean angle of attack (body) is found to be constant for pitch (body) angles between −10 and +40°, the aerodynamic performance of the flies changes marginally in this range of pitch (body) angles. The body is struck by the air from below. Parasite drag (the drag of non-lift-producing parts of the insect) is not minimal in this situation. However, the angle of attack (body) decreases with increasing translation velocity. This leads to a relative reduction in the body drag. A comparison with Nachtigall's (1966), figures 25 and 37) and Vogel's (1967) measurements reveals that the angles of attack (body) that have been found in free flight are consistent with a sufficient usage of aerodynamic lift during flight.

Vogel (1966) and David (1978) have studied forward flight in *Drosophila*. They found relationships among body inclination, flight velocity and angle of attack similar to those described here. But, as they have both recorded only level flight in their wind tunnels, they could not observe the dependence of the ascent angle on the pitch (body) angle. In their experimental situation thrust was linerly related to flight speed and not to the square of speed as would be expected theoretically. This result should not be overemphasized, because flight velocity could not be varied independently of the angle of attack (body) (even in Vogel's own results (figure 5; Vogel 1966) a nonlinear dependence between drag and speed is indicated).

PHILOSOPHICAL TRANSACTIONS OF THE ROYAL SOCIETY B BIOLOGICAL SCIENCES

4.2. *Sideways motion by motor sidethrust?*

In the examples presented here the movements perpendicular to the sagittal plane can be explained without a sidethrust generated by the flight motor. As is shown in the simulation of figure 7, it is sufficient to consider the influence of roll movements and the inertial forces to explain the observed sideways movements. It cannot be excluded, however, that a sidethrust accompanying roll movements is generated. However, even if this would be the case, it seems to be of weak significance. Before the roll movements could be quantitatively measured some manoeuvres could only be explained if a sidethrust generated by the flight motor was assumed (Wagner 1982*b*). These manoeuvres can now be attributed to rolling. Nachtigall (1979) and Blondeau (1981) analysed the flight of the blowfly *Calliphora*. In contrast to the results of this study, both authors describe a sidethrust in these species. However, in the larger fly *Calliphora* the influence of the inertial forces would be expected to last longer than the seven wing-beat cycles (about 43 ms) Nachtigall registered. Since he does not specify the flight manoeuvres before the fly entered the area of filming, his conclusion does not seem compelling. This is true in spite of Nachtigall's observation of phase shifts in the wing beat cycles left and right and different effective 'wing lengths'. Blondeau fixed the flies in a gauge system. If the adjustment was not perfect or if the line of action of the force and moment vector varies with respect to the centre of gravity (Hollick 1940), a sidethrust could occur in the apparatus, although the flies did not generate such a force. This interpretation of Blondeau's results is supported by his own observation of a coupling of yaw and sidethrust in most of the examples he published.

4.3. *Rotations, torques and visual flow*

Although the angular velocities and accelerations, but not the torques, can be derived from the films, the temporal structure of the angular movement allows the deduction of the basic organization of the flight motor. The movements about the three orthogonal axes are controlled independently. Therefore, the torques about the body axes are very probably not coupled. Similarly, Blondeau & Heisenberg (1982) found a three-dimensional optomotor control in *Drosophila* indicating the generation of three independent torque components. These results seem to be contradictory to measurements in tethered flight (Reichardt 1986). However, as Reichardt averaged over many stimulus presentations, the coupling he found could be due to motor patterns of banked turns (figure 3*a*, table 2).

Sometimes the distinction of roll and yaw into two degrees of freedom is regarded as artificial (Pringle 1974; Srinivasan 1977). However, turning about the vertical and long axis can be independently controlled in houseflies. Roll movements play a special role for a flier which does not produce a sidethrust: rolling provides a means to increase manoeuvrability, since it provides the possibility of moving sideways during straight flight. For this purpose yaw and roll must be independent of each other.

During simultaneous rotation and translation the visual flow on the eyes is complex. Although it can in principle be decomposed into pure rotational and translational flows, this is not easy to accomplish (Longuet-Higgins & Prazdny 1980). *Musca* performs marked rotations about the long axis by quick turns, which are separated by periods of only little or no turning (figure 4*e*). Angular movements about the long axis differ from those about the vertical and the transverse axis. The roll movements of the body occur much more frequently than angular movements about the other axes (table 2). However, the fly may roll the head considerably

relative to the body. In fixed flight, *Calliphora* stabilizes its head with respect to the environment during self-motion and motion of the environment (Hengstenberg 1984). It is interesting to observe the same behaviour in free-flying *Musca* (Wagner & Wehrhahn 1986). Thus, the flight behaviour and the coordination of head and body movements may be interpreted as an active reduction of the image flow to its translational components. This part of the flow field contains information about distance, which is used, for example, for landing (Wagner 1982*a*).

The flight tracks presented here show that it is not sufficient to analyse only the movement of the centre of gravity of the flies during tracking and chasing. Since flight direction and body direction differ for most of the time, the position of the target on the retina cannot be determined reliably if only the flight path is known. In addition, almost all significant body rotations of the flies result from the turns described above. During a turn, consecutive values of the angular velocity probably depend on each other. This has consequences for the analysis of pursuit sequences. A continuous correlation between input variables to sensory control systems (the retinal target positon or velocity) and output variables (the torques of the pursuer) will at least imply a mechanism which is not present during pursuit (see also paper II).

4.4. *Flight-motor organization and behaviour*

The aerial behaviour of free-flying syrphid males has been studied by Collett & Land (1975*a*, *b*; 1978; Collett 1980*a*, *b*). The flight motor is organized differently from that of *Musca* in these species. Weis-Fogh (1973) has pointed out that syrphid flies have a separate mechanism for lift production allowing them to hover with a horizontally aligned long axis (see also Ellington 1984). Syrphids show a much greater repertoire of manoeuvres than houseflies. *Syritta* can fly backwards and to the side, thus actively holding a target at a constant position on the eye during pursuit. The stragety of *Syritta* is to shadow the target until it lands on a flower and then pounce on this sitting target. *Musca* cannot behave in this way, because its manoeuvrability is much more restricted. Shadowing is not possible if a target, for example, approaches the fly. Indeed, as will be shown in paper II, *Musca* does not shadow the targets it wants to catch but attacks them and tries to hit them in the air. This seems to be a rather suitable strategy for an insect with a restricted manoeuvrability. Thus, the organization of the flight motor reflects some of the constraints of strategies during aerial pursuit, a behaviour related to sexual reproduction and therefore of great importance for these species.

On the other hand, free-flight behaviour in muscids is quite variable in different species. *Ophyra* will hover beneath landmarks making darts to targets passing by (Paijunen 1982). *Fannia*, the lesser housefly, occupies territories underneath landmarks and shows a very regular pattern of activity (Zeil 1986). *Musca* neither hovers, nor have males been observed to make territorial flights. Most of the time the males sit on the walls and start chasing targets from this position. The flight motor seems to be similar in these species. *Ophyra* hovers with inclined long axis (personal observation). The curved flight of *Fannia* resembles that of *Musca* (Land & Collett 1974). It is an interesting question to ask why animals depending on a similar flight motor show such a variability in behaviour.

I thank Professor Reichardt for enabling me to do this work at the Max-Planck-Institut für biologische Kybernetik, and the Max-Planck-Gesellschaft for financial support. H.-J. Dahmen, M. Egelhaaf, W. Reichardt, C. Wehrhahn and J. Zanker read the text. Their criticism helped me to clarify a lot of topics. I thank K. Götz for discussions. J. Emmerton kindly corrected my

PHILOSOPHICAL TRANSACTIONS OF THE ROYAL SOCIETY B BIOLOGICAL SCIENCES

English and gave valuable hints how to improve it. The 35 mm films that helped much in the understanding of the flies' roll movements were kindly made available to me by C. Wehrhahn, who together with K. Hirschel shot these films. L. Heimburger and I. Geiss, who also typed part of the manuscript, prepared most of the figures. I wish to thank them for their help and patience.

Appendix 1

In this paragraph the mathematics of the transformation and the derivation of the Euler angles are shown for the transformation from the x, y, z system to the x_b, y_b, z_b system (figures 2 and A 1, where $x''' = x_b$, $y''' = y_b$ and $z''' = z_b$).

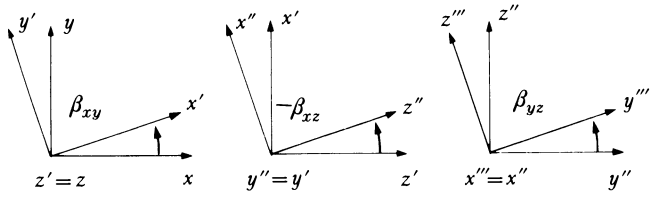

Figure A 1. Reconstruction of the orientation of the fly's body axes in space as described in Appendix 1.

The heading angle β_{xy} is defined as the angle of rotation about the z axis between the x–z plane and the x'–z plane. It ranges from -180 to $+180°$. The pitch (body) angle β_{xz} is the angle of elevation of the x'' axis to the x–y plane (which coincides with the x'–y' plane). It extends from -90 to $+90°$. The roll angle β_{yz} is the angle between the x''–z'' plane and the x'''–z''' plane extending from -180 to $+180°$. All Euler angles are positive in the counterclockwise direction if seen from the positive part of the axis about which they are defined. The pitch (body) angle as used here is the negative value of the corresponding Euler angle. Therefore, in the equations and figure A 1 $-\beta_{xz}$ occurs. Since all coordinate systems were right-handed and cartesian, the transformation matrix is given by the following expression:

$$M = \begin{bmatrix} \cos\beta_{xy}\cdot\cos(-\beta_{xz}) & \sin\beta_{xy}\cdot\cos(-\beta_{xz}) & -\sin(-\beta_{xz}) \\ \cos\beta_{xy}\cdot\sin(-\beta_{xz})\cdot\sin\beta_{yz} - \sin\beta_{xy}\cdot\cos\beta_{yz} & \sin\beta_{xy}\cdot\sin(-\beta_{xz})\cdot\sin\beta_{yz} + \cos\beta_{xy}\cdot\cos\beta_{yz} & \cos(-\beta_{xz})\cdot\sin\beta_{yz} \\ \cos\beta_{xy}\cdot\sin(-\beta_{xz})\cdot\cos\beta_{yz} + \sin\beta_{xy}\cdot\sin\beta_{yz} & \sin\beta_{xy}\cdot\sin(-\beta_{xz})\cdot\cos\beta_{yz} - \cos\beta_{xy}\cdot\sin\beta_{yz} & \cos(-\beta_{xz})\cdot\cos\beta_{yz} \end{bmatrix} \quad \text{(A 1)}$$

The necessary computations for each rotation can be expressed by a 3×3 matrix. The multiplication rule is $M = M(\beta_{yz})\ M(\beta_{xz})\ M(\beta_{xy})$. The transformation from the earth-related coordinate system to the x_b, y_b, z_b system is performed with this matrix.

The points chosen for digitizing the fly's axes lie on the x_b axis (head, abdomen) or y_b axis (wing base left and right), respectively, therefore the angles characterizing the flight posture can be derived in the following way: for the point on the abdomen it holds that

$$P_A = \begin{bmatrix} x_b \\ y_b \\ z_b \end{bmatrix} = \begin{bmatrix} A \\ 0 \\ 0 \end{bmatrix}, \quad \text{(A 2)}$$

then

$$\begin{bmatrix} x \\ y \\ z \end{bmatrix} = M^{-1} \begin{bmatrix} x_b \\ y_b \\ z_b \end{bmatrix} = \begin{bmatrix} \cos \beta_{xy} \cdot \cos(-\beta_{xz}) \\ \sin \beta_{xy} \cdot \cos(-\beta_{xz}) \\ -\sin(-\beta_{xz}) \end{bmatrix} \cdot A. \tag{A 3}$$

Thus

$$\beta_{xy} = \arctan(y, x) \tag{A 4}$$

and

$$\beta_{xz} = \arctan(z, \sqrt{(y^2+x^2)}). \tag{A 5}$$

In the same manner α_{xy}, α_{xz} and γ_{xy} and γ_{xz} were measured. Since in the 16 mm films no information about the roll angle could be obtained, it is worthwhile to state that the heading and the pitch (body) angle, as defined here, can be derived without knowledge of the roll angle.

The computation of the roll angle is not so easy. By inspection of (A 1) one can find a condition for the evaluation of this angle. For the point on the transverse axis P_W holds:

$$P_W = \begin{bmatrix} x_b \\ y_b \\ z_b \end{bmatrix} = \begin{bmatrix} 0 \\ W \\ 0 \end{bmatrix} \tag{A 6}$$

and

$$\begin{bmatrix} x \\ y \\ z \end{bmatrix} = M^{-1} \begin{bmatrix} x_b \\ y_b \\ z_b \end{bmatrix} = \begin{bmatrix} -\sin \beta_{xy} \cdot \cos \beta_{yz} + \cos \beta_{xy} \cdot \sin(-\beta_{xz}) \cdot \sin \beta_{yz} \\ \cos \beta_{xy} \cdot \cos \beta_{yz} + \sin \beta_{xy} \cdot \sin(-\beta_{xz}) \cdot \sin \beta_{yz} \\ \cos(-\beta_{xz}) \cdot \sin \beta_{yz} \end{bmatrix} \cdot W. \tag{A 7}$$

thus,

$$\frac{x^2+y^2}{z^2} = \frac{W^2 \cdot \cos^2 \beta_{yz}}{W^2 \cdot \cos^2(-\beta_{xz}) \cdot \sin^2 \beta_{yz}} + \frac{W^2 \cdot \sin^2 \beta_{yz} \cdot \sin^2(-\beta_{xz})}{W^2 \cdot \cos^2(-\beta_{xz}) \cdot \sin^2 \beta_{yz}}$$

$$= \frac{1}{\cos^2(-\beta_{xz}) \tan^2(\beta_{yz})} + \tan^2(-\beta_{xz}) \tag{A 8}$$

and

$$\tan \beta_{yz} = \frac{z}{\sqrt{[\cos^2(-\beta_{xz})(x^2+y^2) - z^2 \cdot \sin^2(-\beta_{xz})]}},$$

$$\beta_{yz} = \arctan \frac{z}{\sqrt{[\cos^2(-\beta_{xz})(x^2+y^2) - z^2 \cdot \sin^2(\beta_{xz})]}} \tag{A 9}$$

defined from -90 and $+90°$. To compute the roll angle a further step is necessary. This is done by eliminating $\sin(\beta_{yz})$:

$$\sin \beta_{yz} = (x + W \cdot \sin \beta_{xy} \cdot \cos \beta_{yz}) \cdot \frac{1}{W \cdot \cos \beta_{xy} \cdot \sin(-\beta_{xz})} \tag{A 10}$$

$$\sin \beta_{yz} = (y - W \cdot \cos \beta_{xy} \cdot \cos \beta_{yz}) \cdot \frac{1}{W \cdot \sin \beta_{xy} \cdot \sin(-\beta_{xz})} \tag{A 11}$$

$$\frac{x + W \cdot \sin \beta_{xy} \cdot \cos \beta_{yz}}{W \cdot \cos \beta_{xy} \cdot \sin(-\beta_{xz})} = \frac{y - W \cdot \cos \beta_{xy} \cdot \cos \beta_{yz}}{W \cdot \sin \beta_{xy} \cdot \sin(-\beta_{xz})}. \tag{A 12}$$

PHILOSOPHICAL TRANSACTIONS OF THE ROYAL SOCIETY B BIOLOGICAL SCIENCES

β_{yz} can then be derived as

$$-x \cdot \sin \beta_{xy} + y \cdot \cos \beta_{xy} = W \cdot \cos \beta_{yz}$$

$$\cos \beta_{yz} = (y \cdot \cos \beta_{xy} - x \cdot \sin \beta_{xy})/W,$$

$$\beta_{yz} = \arccos [(y \cdot \cos \beta_{xy} - x \cdot \sin \beta_{xy})/W]. \quad \text{(A 13)}$$

This procedure leads to values between 0 and 180°. By combination with the first method the roll angle can be obtained in the range of −180 to +180°. Since the distance of the wing base point to the long axis is only about 1 mm, both wing base points were recorded. The roll angle is the mean of the values left and right. The error introduced by this method of deriving β_{yz} depends on the orientation of the fly to the camera. It amounts to about 2–3° if the fly's long axis is approximately parallel to the y_e-axis, but becomes much greater if it is perpendicular to it. This is the reason why only sequences have been recorded in which the orientation of the fly to the camera was in a range of about $90 \pm 45°$. It is important here to state that the sum of the triade α_{xy}, β_{xy}, γ_{xy} or α_{xz}, β_{xz}, γ_{xz}, respectively, and the diade β_{yz}, γ_{yz} is different from zero, because the angles are derived in coordinate systems of different orientation.

Appendix 2

The algorithm used for simulating sideways motion is considered.

As shown in §3.2.3, the following two components influence sideways motion: (i) roll angle and (ii) inertial forces.

The influence of the roll angle on sideways motion in the 16 mm examples is expressed by the following equation:

$$R_S = \sin (30°)\ V_{3D} \sin (\gamma_{xy}). \quad \text{(A 14)}$$

V_{3D} is the translation velocity and γ_{xy} the angle of sideslip. Sin (30°) V_{3D} is the factor representing the motor force. It is assumed that the force is in first approximation proportional to V_{3D} with an inclination of 30° upward (cf. Götz & Wandel 1984). During curved flight the influence of the roll angle on sideways motion is more complex. Owing to the action of inertial forces the dependence between the roll angle and the sideways motion is influenced. For reasons of simplicity this influence on the effect of rolling is considered with a threshold mechanism. It is assumed that the sign of R_S changes if the angular velocity about the vertical axis and the angle of sideslip are simultaneously greater than a threshold value of 300° per second and 30°, respectively.

The influence of the inertial forces independent of the roll component (I_S) can only be roughly estimated. A dynamic event as a turn is too complex to be exactly described with the information obtained from the films. The simplest 'Ansatz' for the force equation that regards only a constant friction in the forward direction is used here:

$$\boldsymbol{F} = m\dot{v}_f + kw_f \quad \text{(A 15)}$$

where $\dot{v}_f$ is forward acceleration, v_f is forward velocity, k is friction constant and m is mass of the fly (*ca.* 20 mg). The calculation of the sideways movement that results from a turn must take into account the sum of the contributions before the instant regarded. Therefore a convolution is necessary. If one assumes that the force (indicated by flight velocity) remains constant from frame to frame (quasi-steady conditions) and acts only in the direction of the

long axis, the differential equation is equal to the formula given above with $m/k = \tau$. The sideways velocity is assumed to be zero before the beginning of the turn. Then a solution can be given.

$$I_S = \frac{1}{\tau} \sum_{\nu=1}^{m} v_f(\nu)\, e^{\frac{-[m-\nu]}{\tau}} \sin(\alpha_v(\nu)). \quad \text{(A 16)}$$

A multiplication with the factor $\sin(\alpha_v(\nu))$ is necessary, because the sideways velocity is a vector oriented perpendicularly to the long axis. $\alpha_v(\nu)$ is the angle around which the long axis has changed its orientation since the beginning of the turn.

The entire sideways velocity is given by

$$V_S = -AI_S + R_S. \quad \text{(A 17)}$$

For the simulation in figure 7 the following parameters were used: $\tau = 46$ ms; integration time $m = 100$ ms (10 frames); A is a factor which for reasons of simplicity is also set to 46 ms here.

References

Baker, P. S., Gewecke, M. & Cooter, R. J. 1981 The natural flight of the migratory locust, *Locusta migratoria* L. III. Wing-beat frequency, flight speed and attitude. *J. comp. Physiol.* **141**, 233–237.

Blondeau, J. 1981 Aerodynamic capabilities of flies, as revealed by a new technique. *J. exp. Biol.* **92**, 155–163.

Blondeau, J. & Heisenberg, M. 1982 The three-dimensional optomotor torque system of *Drosophila melanogaster*. *J. comp. Physiol.* **145**, 321–329.

Bülthoff, H., Poggio, T. & Wehrhahn, C. 1980 3-D-analysis of the flight trajectories of flies (*Drosophila melanogaster*). *Z. Naturforsch.* C **35**, 811–815.

Collett, T. S. 1980*a* Some operating rules for the optomotor system of a hoverfly during voluntary flight. *J. comp. Physiol.* **138**, 271–282.

Collett, T. S. 1980*b* Angular tracking and the optomotor response. An analysis of visual reflex interaction in a hoverfly. *J. comp. Physiol.* **140**, 145–158.

Collett, T. S. & Land, M. F. 1975*a* Visual control of flight behaviour in the hoverfly, *Syritta pipiens* L. *J. comp. Physiol.* **99**, 1–66.

Collett, T. S. & Land, M. F. 1975*b* Visual spatial memory in a hoverfly. *J. comp. Physiol.* **100**, 59–84.

Collett, T. S. & Land, M. F. 1978 How hoverflies compute interception courses. *J. comp. Physiol.* **125**, 191–204.

David, C. T. 1978 The relationship between body angle and flight speed in free-flying *Drosophila*. *Phys. Entomol.* **3**, 191–195.

David, C. T. 1984 The dynamics of height stabilization in *Drosophila*. *Physiol. Ent.* **9**, 377–386.

Egelhaaf, M. 1985 Towards the neuronal basis of figure-ground discrimination by relative motion in the visual system of the fly. Doctoral thesis, University of Tübingen.

Ellington, C. P. 1984 The aerodynamics of hovering insect flight. *Phil. Trans. R. Soc. Lond.* B **305**, 1–181.

Esch, H., Nachtigall, W. & Kogge, S. N. 1975 Correlations between aerodynamic output, electrical activity in the indirect flight muscles and wing positions of bees flying in a servomechanically controlled wind tunnel. *J. comp. Physiol.* **100**, 147–159.

Fifer, S. 1961 *Analogue computation*, vol. 4. New York, Toronto, London: McGraw Hill.

Gettrup, E. & Wilson, D. M. 1964 The lift-control reaction of flying locusts. *J. exp. Biol.* **41**, 183–190.

Götz, K. G. 1968 Flight control in *Drosophila* by visual perception of motion. *Kybernetik* **4**, 199–208.

Götz, K. G. 1983 Bewegungssehen und Flugsteuerung bei der Fliege *Drosophila*. In *Biona-Report*, 2. *Akademie der Wissenschaften und der Literatur zu Mainz*, *S.* (ed. W. Nachtigall), pp. 21–33. Stuttgart, New York: G. Fischer.

Götz, K. G. & Wandel, U. 1984 Optomotor control of the force of flight in *Drosophila* and *Musca*. II. Covariance of lift and thrust in still air. *Biol. Cybern.* **51**, 135–139.

Heide, G. 1979 Proprioceptive feedback dominates the central oscillator in the patterning of the flight motoneuron output in *Tipula* (*Diptera*). *J. comp. Physiol.* **134**, 177–189.

Hengstenberg, R. 1984 Roll-stabilization during flight of the blowfly's head and body by mechanical and visual cues. In *Localization and orientation in biology and engineering* (ed. D. Varju & H. U. Schnitzler), pp. 121–134. Berlin, Heidelberg: Springer-Verlag.

Hollick, F. S. J. 1940 The flight of the dipterous fly *Muscina stabulans* Fallen. *Phil. Trans. R. Soc. Lond.* B **230**, 357–390.

Land, M. F. & Collett, T. S. 1974 Chasing behaviour of houseflies (*Fannia canicularis*). *J. comp. Physiol.* **89**, 331–357.

Longuet-Higgins, H. G. & Prazdny, K. 1980 The interpretation of a moving retinal image. *Proc. R. Soc. Lond.* B **208**, 385–397.

PHILOSOPHICAL TRANSACTIONS OF THE ROYAL SOCIETY B BIOLOGICAL SCIENCES

Nachtigall, W. 1966 Die Kinematik der Schlagflügelbewegungen von Dipteren. Methodische und analytische Grundlagen zur Biophysik des Insektenflugs. *Z. vgl. Physiol.* **52**, 155–211.
Nachtigall, W. 1979 Schiebeflug bei der Schmeissfliege *Calliphora erytheocephala* (Diptera: Calliphoridae). *Ent. gen.* **5** (3), 255–265.
Nachtigall, W. (ed.) 1983 *Biona report 1 and 2, Akademie der Wissenschaften und der Literatur zu Mainz*. Stuttgart, New York: G. Fischer.
Nachtigall, W. & Roth, W. 1983 Correlations between stationary measurable parameters of wing movement and aerodynamic force production in the blowfly (*Calliphora vicina* R.-D.). *J. comp. Physiol.* **150**, 251–260.
Pajunen, I. 1982 Swarming behaviour in *Ophyra leucostoma* Wied. (Diptera, Muscidae). *Ann. zool. fenn.* **19**, 81–85.
Poggio, T. & Reichardt, W. 1981 Visual fixation and tracking by flies: mathematical properties of simple control systems. *Biol. Cybern.* **44**, 101–112.
Pringle, J. W. S. 1974 Locomotion: flight. In *The physiology of Insecta* (ed. M. Rockstein), 2nd edn, vol. 3, pp. 433–475. New York, London: Academic Press.
Rainey, R. C. (ed.) 1976 *Insect flight*. Oxford, London, Edinburgh, Melbourne: Blackwell Scientific Publications.
Reichardt, W. 1986 (in preparation.)
Reichardt, W. & Poggio, T. 1976 Visual control of orientation behaviour in the fly. I. A quantitative analysis. *Q. Rev. Biophys.* **9**, 311–375.
Spüler, M. & Heide, G. 1978 Simultaneous recordings of torque, thrust and muscle spikes from the fly *Musca domestica* during optomotor responses. *Z. Naturforsch.* **33**C, 455–457.
Srinivasan, M. V. 1977 A visually evoked roll response in the housefly. Open-loop and closed-loop studies. *J. comp. Physiol.* **119**, 1–14.
Vogel, S. 1966 Flight in *Drosophila*. I. Flight performance of tethered flies. *J. exp. Biol.* **44**, 567–578.
Vogel, S. 1967 Flight in *Drosophila*. III. Aerodynamic characteristics of fly wings and wing models. *J. exp. Biol.* **46**, 431–443.
Wagner, H. 1980 Messung und Beschreibung von Landetrajektorien der Stubenfliege (*Musca domestica*, L.). Diplomarbeit der Universität Tübingen.
Wagner, H. 1983*a* Flow-field variables trigger landing in flies. *Nature Lond.* **297**, 147–148.
Wagner, H. 1982*b* Aspekte der Kinematik und der visuellen Orientierung bei freifliegenden Stubenfliegenweibchen (*Musca domestica* L.). *Verh. Dtsch. Zool. Ges.* 1982, 338.
Wagner, H. & Wehrhahn, C. 1986 (In preparation.)
Wehner, R. 1981 Spatial vision in arthropods. In *Handbook of Sensory Physiology* (ed. H. Autrum), vol. VII/6c, pp. 288–616. Berlin, Heidelberg, New York: Springer Verlag.
Wehrhahn, C., Poggio, T. & Bülthoff, H. 1982 Tracking and chasing in houseflies (*Musca*). An analysis of 3-D flight trajectories. *Biol. Cybern.* **45**, 123–130.
Wehrhahn, C. & Reichardt, W. 1975 Visually induced height orientation of the fly *Musca domestica*. *Biol. Cybern.* **20**, 37–50.
Weis-Fogh, T. & Jensen, M. 1956 Biology and physics of Locust flight. I. Basic principles in insect flight. A critical review. *Phil. Trans. R. Soc. Lond.* B **239**, 415–457.
Weis-Fogh, T. 1973 Quick estimates of flight fitness in hovering animals, including novel mechanisms for lift production. *J. exp. Biol.* **59**, 169–230.
Wendler, G. 1978 Lokomotion: das Ergebnis zentral-peripherer Interaktion. *Verh. dt. Zool. Ges.* pp. 80–96.
Zeil, J. 1983 Sexual dimorphism in the visual system of flies: The free flight behaviour of male Bibionidae (Diptera). *J. comp. Physiol.* **150**, 395–412.
Zeil, J. 1986 (In preparation.)

PHILOSOPHICAL TRANSACTIONS OF THE ROYAL SOCIETY B BIOLOGICAL SCIENCES